10.18462/iir.gl.2018.1217

EJECTOR CHARACTERIZATION FOR REFRIGERATION APPLICATIONS WITH NATURAL REFRIGERANTS

A. Milazzo[a]*, M.A. Coppola[b], G. Cortella[b], P. D'Agaro[b], F. Giacomelli[a],

[(a)] University of Firenze (DIEF) Firenze, Italy

[(b)] University of Udine (DPIA) Udine, Italy

[(*)] *Corresponding author, adriano.milazzo@unifi.it*

ABSTRACT

Employing natural fluids in refrigerating plants at warm climate conditions sometimes impacts negatively on the system performance. Ejectors can play a key role in configurations aiming at improving the efficiency of such systems, however their geometry has to be optimized in order to gain the best benefit. Scope of this work is a numerical investigation on the geometry of the ejector in a cascade plant configuration with natural refrigerants, aiming at identifying the influence of various geometry aspects on the performance of the system. A one-dimensional model is employed for the ejector, while the performance of the refrigerating plant is evaluated in different operating conditions in order to seek the optimal configuration.

Keywords: Ejector, Carbon Dioxide, Ammonia, Cascade, Natural refrigerants

1. INTRODUCTION

Ejectors are proposed from several decades to reduce throttling losses in the refrigeration cycle, by performing work recovery. Recently they have been put in the spotlight to increase the global efficiency of CO_2 refrigerating units (Elbel and Hrnjak (2008), Gullo *et al* (2017), Haida *et al* (2016)), but the first applications were proposed many decades before (Gay (1931)). A comparison between various configurations can be found as an example in Lawrence and Elbel (2013). One of the main concerns is their design, which requires specific modelling skills. A model is presented in this paper, for a two phase ejector applied to a refrigerating cycle at two evaporating temperatures. This configuration can be successfully used for all those applications where the refrigerating effect can be exploited at two temperature levels, thus improving the exergy efficiency. This is the case of blast freezers where air is subject to a significant temperature difference between inlet and outlet of the refrigerating coil.

2. EJECTOR MODEL

An early attempt to model a two-phase ejector for expansion loss recovery in refrigeration applications was presented by Kornhauser (1990). Several low-pressure refrigerants were simulated via a homogeneous equilibrium model. A review of the various proposals for modelling this kind of ejectors may be found in Elbel (2011). More recently, Banasiak and Hafner (2011) presented a detailed description of a 1-d model specifically conceived for expansion work recovery in CO_2 refrigeration systems.
Given that the specific objective of the present work is a design optimization, a design procedure is needed rather than a performance calculation. Therefore, instead of fixing an ejector geometry and evaluating its performance in different working conditions, one should design a different ejector for each condition. The model used in this paper is an evolution of previous work by Grazzini *et al* (2012) and relies on the CRMC criterion (Eames, 2002). According to this criterion, a Constant Rate of Momentum Change is fixed for the diffuser. Hence, for a given flow rate, the deceleration rate dw/dz along the axis is known. From this datum, it's easy to write explicitly the fundamental flow relations for a horizontal duct without heat or work exchange:

$$\frac{dh}{dz} = w\frac{dw}{dz} \qquad (1)$$

$$\frac{dP}{dz} = -\rho w \frac{dw}{dz} - \left(\frac{dP}{dz}\right)_f \quad (2)$$

$$A(z) = \frac{\dot{m}}{\rho w} \quad (3)$$

Conservation of energy (Eq. 1) gives directly the enthalpy variation, while the equation of mechanical energy (2) gives the pressure variation. The last term in Eq. 2 introduces a pressure loss due to viscous dissipation, not included in the original CRMC method. An equation of state in the form $\rho = \rho(P,h)$ is needed in order to solve continuity equation (3) that finally gives the flow section *A*. The original work by Eames (2002) used an ideal gas equation, while here we rely on NIST Refprop functions. Once a flow rate $\dot{m}$ and a set of initial conditions are specified, these equations allows to design a continuous profile for the duct and also to evaluate the fluid conditions at exit. The deceleration rate dw/dz should have a moderate value, in order to avoid exceedingly sharp diameter variations, especially for the diverging ducts, that otherwise would suffer from flow recirculation. On the other hand, increasing the duct length increases the viscous dissipation and hence a compromise must be sought.

The same set of equations may be used for a supersonic nozzle. In this case we must fix an acceleration rate low enough to fulfil the well known rules for the diverging part after the nozzle throat.

The nozzle and diffuser profiles designed in this way are not necessarily optimal in terms of efficiency or easy to manufacture. They are just used here to give a design that complies with the limit fluid accelerations and decelerations and hence gives a duct length (i.e. a friction loss) which is proportionate to the boundary conditions. On the other hand, the widespread literature on ejectors (e.g. Huang *et al*, 1999), customarily uses fixed values for the nozzle and diffuser efficiencies, unrelated to the expansion / compression ratio. Even if these efficiency values are carefully calibrated against some experimental result, their extrapolation to different conditions is questionable.

Another problem may concern the fluid properties, that are calculated by NIST functions at thermodynamic equilibrium. In the case of a two-phase ejector, one should account for the occurrence of metastable conditions. However, this introduces further parameters that need experimental validation and eventually reduce the model reliability. Therefore, a simple equilibrium approach is preferred and the results are checked against published experimental results in terms of global ejector performance.

The pressure loss term in Eq. 2, for a single phase flow, may be calculated through a friction factor *f*

$$\left(\frac{dP}{dz}\right)_f = f\,\frac{\rho w^2}{2D} \quad (4)$$

which may be calculated through the classic Churchill correlation (Churchill, 1977). For two phase flow, we may use the correlation introduced by Muller-Steinhagen and Heck (1986), linking the pressure loss to the vapour quality *x*:

$$\left(\frac{dP}{dz}\right)_{f,tp} = G(1-x)^{1/C} + Bx^C \quad (5)$$

where

$$G = A + 2(B-A)x \quad A = \left(\frac{dP}{dz}\right)_{f,\lambda} = f_l \frac{M}{2\rho_\lambda D} \;;\; B = \left(\frac{dP}{dz}\right)_{f,v} = f_v \frac{M}{2\rho_v D} \quad (6)$$

and $M = \rho w$ is the mass velocity of the two-phase flow. Again, liquid and vapour friction factors are calculated through the Churchill correlation.

What has been said is valid only for a mono-dimensional flow. A different approach is needed for the mixing zone, where motive and entrained flows travel with highly different velocities and momentum is transferred from the fast to the slow current. Here we simply rely on a mixing efficiency, defined as:

$$w_{mix} = \eta_{mix} \frac{w_m + \omega w_e}{1+\omega} \quad (7)$$

where w_m, w_e and w_{mix} are the motive, entrained and mixed flow velocities while ω is the entrainment ratio, i.e. the ratio between entrained and motive mass flow rates. The mixing section is assumed at constant pressure, according to the prevailing approach (Besagni *et al*, 2016).

The ejector model needs the fluid conditions at the two inlets (motive and entrained flows). Low velocities (e.g. 10 m s^{-1}) are assumed in these sections. The mixing section is basically at the same pressure of the entrained flow inlet, as no significant acceleration of this flow is foreseen before it comes in contact with the motive flow at the nozzle exit. Therefore, we know the inlet conditions and the exit pressure for the motive nozzle, and the model is able to design it and calculate the exit conditions.
A trial value of entrainment ratio is hence assumed and a mixed flow velocity is calculated by Eq. 7. An energy balance across the mixing zone yields the stagnation enthalpy of the mixed flow:

$$h_{0,mix} = \frac{h_{0,m} + \omega h_{0,e}}{1+\omega} \tag{8}$$

whence the static enthalpy of the mixed flow may be evaluated.
At this point, the inlet conditions for the diffuser are ready. The exit condition may be found by imposing that a suitable minimum velocity is still present at the diffuser exit and pressure and enthalpy can be evaluated accordingly. If exit pressure is given, e.g. when the diffuser exit is connected to a heat exchanger where a phase change occurs at fixed temperature, one may adjust the trial value of the entrainment ratio until the condition on the diffuser exit velocity is satisfied.
Common input data used for the ejector model are summarized in Table 1.

Table 1. Model input data

Relative wall roughness for all ducts (used in Churchill's formula)	ε / D	0.001
Mixing efficiency	η_{mix}	0.85
Fluid velocity at ejector inlets and outlet	w_{min}	10 m s^{-1}
Acceleration rate in the nozzle	dw/dz	4000 s^{-1}
Deceleration rate in the diffuser	dw/dz	80 s^{-1}

The model has been validated against experimental data reported by Banasiak *et al* (2015), setting the same conditions at nozzle inlet (e.g 25°C, 7.2 MPa) and flow rate (0.04 kg s^{-1}). The nozzle throat diameter calculated by our model is equal (1 mm) to the value reported in Banasiak *et al* (2015). Furthermore, as will be shown later, the ejector efficiency gives similar values. Unfortunately, most authors concentrate on trans-critical systems, while here we consider a sub-critical cycle within a cascade system, yielding quite different working conditions. In any case, the model is suitable as a tool for comparative evaluations within a well defined range of solutions.

3. EJECTOR CYCLE AND APPLICATION

A possible application of the two-phase ejector described above is analysed, putting in evidence the gain in efficiency directly through the COP achieved with respect to the same cycle without the use of the ejector. An important feature is that the correct geometry (or more precisely the sizing) is chosen compatibly with other system components, such as the evaporators.
In this paper we focus our attention on a cycle proposed by Oshitani et al. (2005), in which the two-phase flow discharged from the ejector is sent to a second evaporator, which leads directly to the compressor. This cycle differs from the standard one in that it does not require a liquid-vapour separator and allows for evaporation at two different temperatures. This ejector cycle is called a COS (Condenser Outlet Split) because the liquid is split at the condenser outlet. A schematic diagram of the COS ejector cycle, low stage of a cascade configuration, is shown in Fig. 1 and the corresponding (*P*-*h*) diagram in Fig. 2. In this case a CO_2 (R744) COS cycle has been considered, as the low stage (LS) of a cascade cycle with the higher stage (HS) working with ammonia (R717). A cascade cycle has been chosen to better exploit the good performance of CO_2 refrigerating cycles at subcritical operation mode.
An application of this kind of cycle could be in an air blast freezer, where air is brought to the freezing temperature by the two evaporators, first passing through the higher temperature one and then in the lower temperature one, in which the temperature is free to be adequately set to meet the necessary requirements.
The cascade cycle considered has been modelled with EES (EES, 2018), at steady state conditions, neglecting pressure drops and heat loss. The efficiency of the compressors η_{cp} is provided by exemplary correlations obtained from manufacturer data (Bitzer).

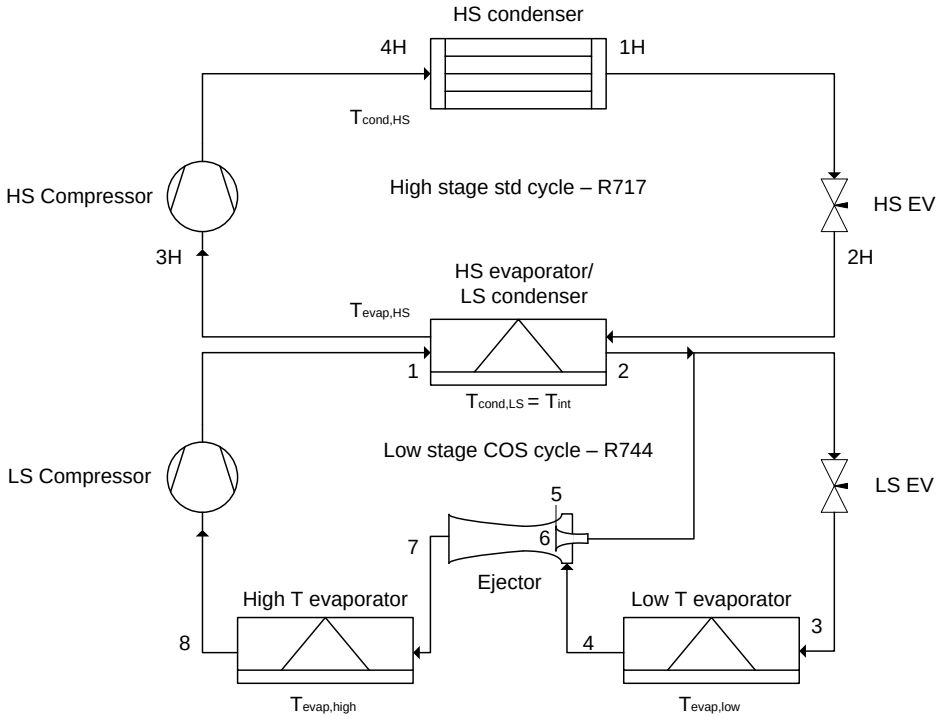

Fig 1. Schematic diagram of the cascade (LS COS cycle + HS STND cycle).

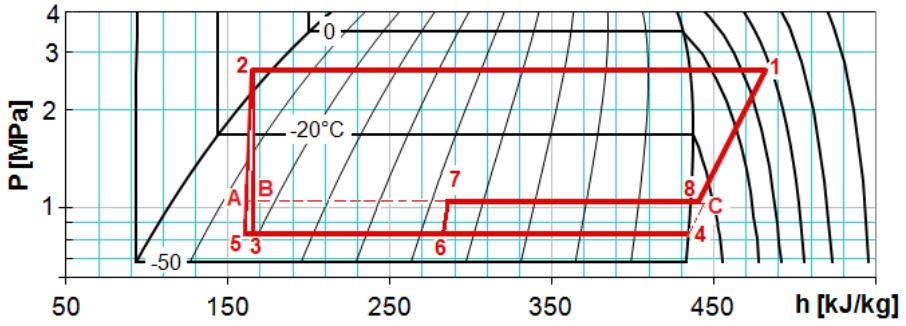

Fig 2. *p-h* diagram of the LS COS cycle.

4. THERMODYNAMIC CYCLE MODEL

The $T_{evap,low}$ is set at -45°C and the cooling load considered is 20 kW. The intermediate temperature T_{int} varies in a range between 0°C and -15°C in order to evaluate the most favourable value. The lower this temperature, the less energy is available in the motive stream of the ejector. An outdoor temperature T_{ext} has been chosen equal to 20°C for all the simulations. Appropriate amounts of subcooling and super heating are assumed at the outlets of the exchangers. System operating parameters used in the thermodynamic cycle model are reported in Table 2.

Table 2. System operating parameters

Parameter	Value	Unit
$T_{evap,low}$	-45	°C
Q	20	kW
ΔT_{SH}	5	K
$\Delta T_{SC,LS}$ / $\Delta T_{SC,HS}$	5/2	K
T_{int} ($T_{cond.LS}$)	0, -5, -10, -15	°C
ΔT_{app} (Evaporator/Condenser)	5	K

In the R744 low stage cycle, the motive nozzle efficiency is calculated with the ejector model and is defined as:

$$\eta_{mn} = \frac{h_5 - h_2}{h_5^{isen} - h_2} \quad (9)$$

Furthermore, for comparison with the literature, the ejector efficiency is calculated according to Elbel and Hrnjak (2008) as:

$$\eta_{ej} = \omega \frac{h_C - h_4}{h_B - h_A} \quad (10)$$

where the point numbering is shown in Fig.2 .
The compressor efficiency of both stages is expressed as a function of the compression ratio elaborated at each stage, through the following correlations (Bitzer, 2017):

$$\eta_{cp,LS} = -0.017\beta_{LS}^2 + 0.095\beta_{LS} + 0.52 \quad (11)$$

$$\eta_{cp,HS} = -0.026\beta_{HS}^2 + 0.206\beta_{HS} + 0.342 \quad (12)$$

The temperature $T_{evap,high}$ of the high T evaporator of the COS cycle is determined via the pressure achieved at the exit of the ejector, which in turn is determined by β_{ej} that results from the ejector simulations.
The COP is calculated for the two stages and for the entire cascade configuration with the following expressions:

$$COP_{LS} = \frac{Q_{evap,LS}}{W_{cp,LS}} \qquad COP_{HS} = \frac{Q_{evap,HS}}{W_{cp,HS}} \qquad COP_{glob} = \frac{Q_{evap,LS}}{W_{cp,LS} + W_{cp,HS}} \quad (13)$$

$Q_{evap,LS}$ is the sum of the cooling loads at the low T and high T evaporators. They are functions of the ejector parameters ω and β_{ej} as these two values determine the suction and total flow rates along with the enthalpy at the entrance of the high T evaporator (ejector outlet state).
Ejector entrainment ratio, compression ratio and efficiency values are calculated by the ejector model for a specific geometry at the given condensing temperature. These values are inputs for the cascade system model. As a consequence, the cycle efficiency is calculated for each T_{int}, allowing to seek the best choice.

5. RESULTS AND DISCUSSION

The primary nozzle design, for a given low temperature evaporator condition, is a function of T_{int}. An example is given in Fig. 3 for T_{int} = -10°C. The nozzle shape is not far from a simple convergent-divergent, due to the sharp increase in specific volume at the onset of flashing evaporation. This point actually defines the position of the nozzle throat. The assumed acceleration rate (see Table 1) produces a length of about 22 mm and a half angle of the divergent part of 1.2°. The throat diameter is 1.33 mm.

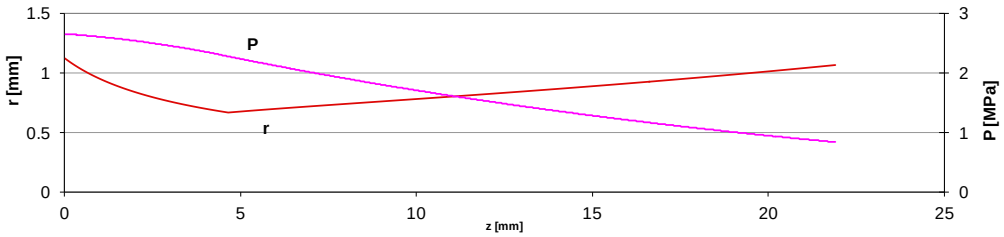

Fig. 3. Primary nozzle radius and pressure profile for T_{int} = -10°C

The pressure profile, shown in the same figure, is very smooth. As T_{int}, increases, the nozzle becomes longer, the throat diameter reduces and nozzle efficiency decreases from 0.889 at T_{int} = -15°C to 0.841 at T_{int} = 0°C. The values are rather low, due to the high friction encountered by the two-phase flow.
The diffuser, on the other hand, has a size and shape that varies according to the exit condition. Given the fixed $T_{evap,low}$ = -45°C, $T_{evap,high}$ has been varied from -44.5 to -39°C, increasing the compression ratio β from 1.02 to 1.25. In any case, the diffuser is completely subsonic and hence has a divergent (practically conical) shape. The dimensions and the efficiency of the diffuser are shown as a function of the compression ratio in Fig. 4. As the length increases, the efficiency decreases due to friction. The divergence angle has approximately the same value as for the nozzle.

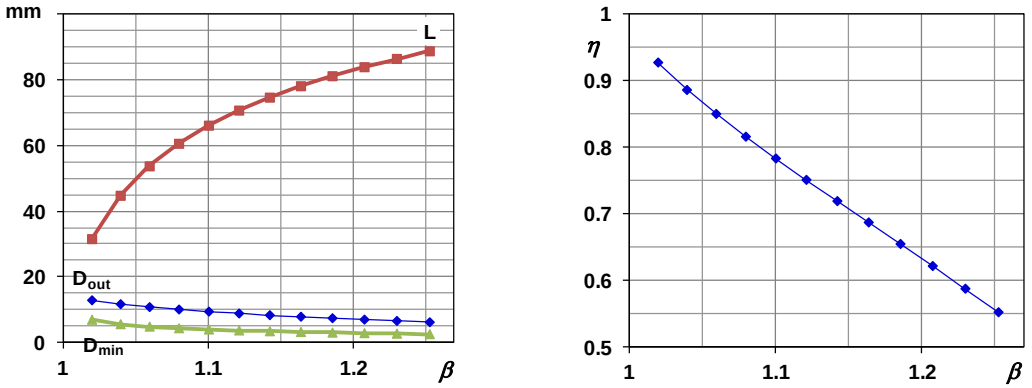

Fig. 4. Diffuser dimensions and efficiency as a function of compression ratio for T_{int} = -10°C

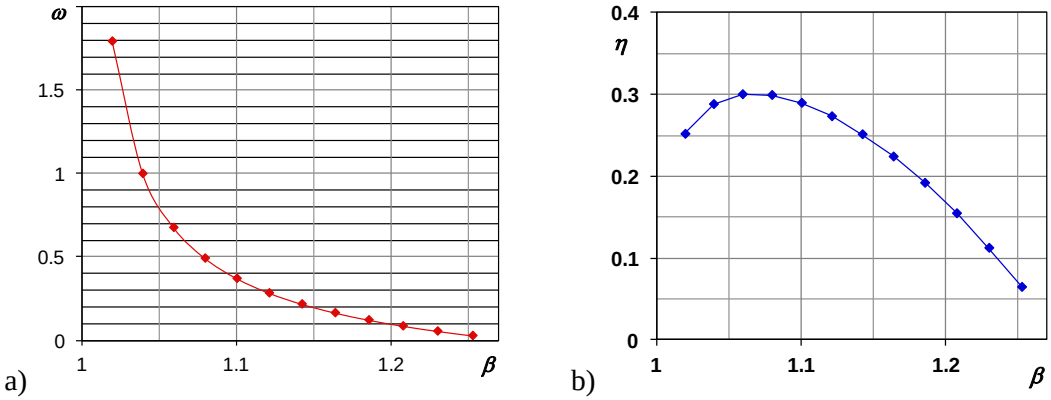

a) b)

Fig. 5. Entrainment ratio (a) and efficiency (b) as a function of compression ratio for T_{int} = -10°C

The entrainment ratio decreases with the compression ratio as shown in Fig. 5a. The ejector efficiency (Eq. 11) is shown in Fig. 5b. The values agree with those reported by Banasiak (2015).

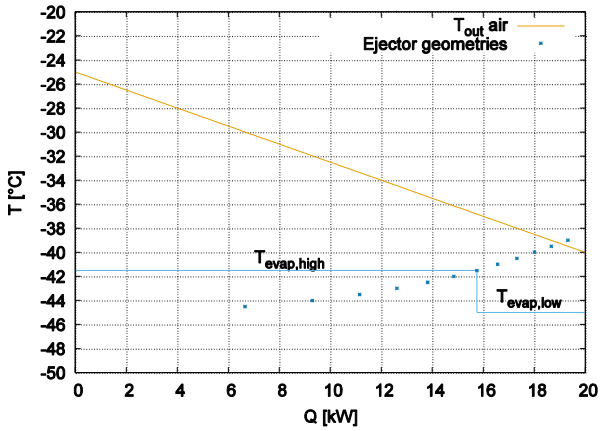

Figure 6 – Temperature profiles in the two evaporators, for T_{int}=-5°C. The blue step indicates the boundary between the first and the second one, while the dots correspond to each ejector geometry.

As an example of the interaction between the ejector and the R744 COS cycle, for T_{int}=-5°C, Fig. 6 shows the high temperature evaporator outlet air temperature against the heat removed in such exchanger. The remaining heat, up to the total of 20 kW, is removed in the low temperature evaporator. The blue points correspond to each ejector's operation point ω and β_{ej}, and the step defines the transition of the evaporation temperature from the first to the second evaporator. The step is chosen for the couple ω and β_{ej}, , that respects an approach temperature of around 5 K in the exchanger, engineering limit imposed in this analysis. From a comparison with the standard cycle performances, carried out for the three T_{int} considered, it results that the ejector COS cycle is always advantageous in terms of COP. It is reasonable to focus on the comparison of the COP with the most favourable case for the standard cycle. Actually, it results that the

intermediate temperature that maximises the COP of the standard cycle is around -11°C. The performance enhancement yielded by the ejector in the COS cycle is around 10%, for T_{int}=-10°C.

Table 3. Comparison of performance coefficients between STND and COS cycles.

T_{int} [°C]	*COP*	Standard cascade cycle	Ejector cascade	Ejector COS performance enhancement [%]
0	COP_{LS}	2.25	2.72	+20.9
	COP_{glob}	1.42	1.64	+15.5
-5	COP_{LS}	2.72	3.26	+19.8
	COP_{glob}	1.53	1.73	+13.1
-10	COP_{LS}	3.28	3.86	+17.7
	COP_{glob}	1.59	1.75	+10.1
-15	COP_{LS}	3.99	4.72	+18.3
	COP_{glob}	1.56	1.70	+9.0

It can be noticed that, due to the performance of the ejector, the highest COP_{glob} is achieved for T_{int}=-10°C, in both cycles, while the highest gain in performance is obtained when T_{int} is higher. This happens because the ejector works better with higher condensing temperatures that correspond to higher energy in the motive nozzle.

6. CONCLUSIONS

Ejectors for expansion work recovery may be a useful complement for a CO2 cycle even if this latter is used as bottom cycle in a cascade configuration.

A CRMC thermodynamic modeling of the ejector shows that the efficiency of this device should be evaluated accounting for the working conditions imposed by the system architecture. In general, the energy losses in the ejector components increase with the pressure ratios. This has been proven in this paper for the motive nozzle and for the diffuser, while the mixing zone has been modeled with a constant efficiency and would deserve further analysis. The global efficiency of the ejector defined by Elbel and Hrjnak (2008) has a maximum for an optimal value of the compression ratio.

The performance gain due to the ejector increases as the temperature lift faced by the CO_2 cycle increases. However, the global COP decreases with the CO_2 cycle temperature lift, as the ammonia top cycle has a better COP. Therefore, a clear optimum exists for the intermediate temperature.

Further analysis of the influence of such temperature, in order to evaluate the functioning of the system the whole year round, and thus to estimate the yearly optimal geometry of the ejector and intermediate temperature, is being carried out.

ACKNOWLEDGEMENTS

The research leading to these results has received funding from the MIUR of Italy within the framework of PRIN2015 project «Clean Heating and Cooling Technologies for an Energy Efficient Smart Grid».

NOMENCLATURE

A	Flow section [m^2]	Greek symbols		*high*	High temp. evaporator
A, B, G	Coefficients eq.	β	Compression ratio	HS	High Stage of cascade
COP	Coeff. Of Performance	ε	Wall roughness [m]	*int*	Intermediate
COS	Condenser Outlet Split	η	Efficiency	*isen*	Isentropic
D	Diameter [m]	ρ	Density [kg m^{-3}]	ℓ	Liquid
f	Friction factor	ω	Entrainment ratio	*low*	Low temp. evaporator
h	Enthalpy [kJ/kg]	*Subscripts*		LS	Low Stage of cascade
$\dot{m}$	Flow rate [kg/h]	*app*	Approach between	*mn*	Motive nozzle

P	Pressure [MPa]		Condenser end Evap.	*SC*	Subcooling
Q	Cooling load [kW]	*cp*	Compressor	*SH*	Superheating
T	Temperature [°C]	*e*	entrained	STND	Standard cycle
w	Velocity [m s^{-1}]	*ej*	Ejector	*tot*	Total
W	Power [kW]	*ext*	External	*tp*	Two-phase
z	Axial coordinate [m]	*evap*	Evaporating	*v*	Vapor
		glob	Global		

REFERENCES

Banasiak, K., Hafner A., 2011. 1D Computational model of a two-phase R744 ejector for expansion work recovery, Int. J. Thermal Sciences, 50, 2235-2247.

Banasiak K., Hafner A., Kriezi E., Madsen K.B., Birkelund M., Fredslund K., Olsson R., 2015. Development and performance mapping of a multiejector expansion work recovery pack for R744 vapour compression units, Int. J. Refrig. 57, 265-276

Besagni G., Mereu R., Inzoli F., Ejector refrigeration: A comprehensive review, Renewable and Sustainable Energy Reviews 53 (2016) 373–407

Bitzer, 2017. BITZER v6.7.0 rev1852 – Available at: https://www.bitzer.de/websoftware/ .

Churchill, S.W. 1977. Friction-factor equation spans all fluid-flow regimes. Chem. Eng. 7, 91-92

Eames, I.W. 2002. A new prescription for the design of supersonic jet-pumps: the constant rate of momentum change method. Appl. Therm. Eng. 22, 121-131.

EES 2018, Engineering Equation Solver, v. 10.268. http://www.fchart.com/ees/.

Elbel, S., Hrnjak, P., 2008. Experimental validation of a prototype ejector designed to reduce throttling losses encountered in transcritical R744 system operation. Int. J. Refrig. 31, 411–422.

Elbel, S., 2011. Historical and present developments of ejector refrigeration systems with emphasis on transcritical carbon dioxide air-conditioning applications, Int. J. Refrig., 34 (7), 1545-1561.

Gay, N.H., 1931. Refrigerating System. U.S. 1,836,318

Grazzini, G., Milazzo, A., Paganini, 2012. D. Design of an ejector cycle refrigeration system. Energy Convers. Manag., 54, 38-46.

Gullo P., Hafner A., Cortella G., 2017. Multi-ejector R744 booster refrigerating plants and air conditioning system integration - A theoretical evaluation of energy benefits for supermarket applications. Int. J. Refrig., 75:164-176.

Haida, M., Banasiak, K., Smolka, J., Hafner, A., Eikevik, T.M., 2016. Experimental analysis of R744 vapour compression rack equipped with multi-ejector expansion work recovery module. Int. J. Refrig. 64, 93–107.

Huang, B.J., Chang, J.M., Wang, C.P., Petrenko, V.A. 1999. A 1-D analysis of ejector performance. Int. J. Refrig. 22, 354-364.

Kornhauser, A.A., 1990. The Use of an Ejector as a Refrigerant Expander, International Refrigeration and Air Conditioning Conference, Purdue University, http://docs.lib.purdue.edu/iracc/82

Lawrence, N., Elbel, S., 2013. Theoretical and practical comparison of two-phase ejector refrigeration cycles including First and Second Law analysis, Int. J. Refrig., 36(4), pp. 1220-1232

Muller Steinhagen H., Heck, 1986. A Simple Friction Pressure Drop Correlation for Two-Phase Flow in Pipes. Chem. Eng. Process., 20 (1986) 297-308

Oshitani, H., Yamanaka, Y., Takeuchi, H., Kusano, K., Ikegami, M., Takano, Y., Ishizaka, N., Sugiura, T., 2005. Vapor Compression Cycle Having Ejector. U.S. Patent Application Publication US 2005/0268644 A1.